High Resolution Ka-band Backscattering Measurement of Deciduous and Coniferous Tree

Wei-An Chuang[1], **Hsuan Ren**[1,2], **Kuan-Liang Chen**[1], **and Jhih-Syuan Huang**[1]

[1]Institute of Space Science, National Central University, Taiwan
[2]Center for Space and Remote Sensing Research, National Central University, Taiwan

Abstract— In this paper, we present Ka-band backscattering measurement of deciduous and coniferous pine trees on National Central University (NCU) campus. The coherent radar system, designed and configured based on a vector network analyzer N5245A PNA-X (10 MHz–50 GHz) is capable of measuring the return power from 26.5 GHz to 50 GHz for VV, HH, HV polarizations at incidence angles between 30 and 80 degrees. In measuring process, the radar system has typical trace of the frequency ranges from 28 to 38 GHz of the received power for a given footprint of tree canopy. For this high resolution, the wind-induced Doppler effects can be ignored. Undesired returns from outside the antenna beam volume are conveniently rejected by gating in time domain. By this feature, the propagating depth through the tree can also be precisely determined so that the effective propagation constant and attenuation factor can be estimated. A reference measurement was taken at normal incidence using a conducting sphere as a calibration target. The calibration was conducted both in anechoic chamber and in-situ measurements. Ensemble average of 2000 samples was taken to estimate the mean return power and later by inverting the radar equation to obtain the backscattering coefficient as functions of frequencies and incident angles are then estimated. To simplify the matrix inversion, a narrow beam is realized with dish antenna. Based on the measured results, backscattering characteristics and statistical properties were analyzed for the cases of deciduous (banyan) and coniferous (pine) trees.

1. INTRODUCTION

A number of research efforts intend at characterizing propagation and backscattering in tree canopies have been reported in the past [1–4]. In Section 2, the inversion of backscattering from measured return power is presented. Those include narrow beam approximation, normalized average power for determining and the reference measurement using a spherical conducting as a target in anechoic chamber. The backscattering measurements of banyan and pine tree on National Central University (NCU) campus made at Ka band, its results at 28 GHz to 38 GHz are presented in Section 3. Based on the measured results,backscattering coefficients characteristics were analyzed for the cases of deciduous (banyan) and coniferous (pine). Finally, examples of recent experimental observations and preliminary results are discussed.

2. INVERSION OF σ° (SCATTERING COEFFICIENT) FROM RETURN POWER

It complements remote sensing in many important areas such as a geological sensing, forest biomass assessment, and so forth. After microwave remote sensing science study began to mature in the late 1970s [5], backscattering enhancement, cross polarization effects, probability density function, and radar remote sensing appeared in the 1980s [6–9]. The development of microwave scattering models appeared in the late 2010s [10]. The backscattering from measurement return power is described by backscattering coefficient (backscattering cross section per unit area). Those include narrow beam approximation, normalized average power for determining and the reference measurement using a spherical conducting as a target in anechoic chamber.

The overage power returned, P_r, is a function of several parameters. It may express as a function of the measured system, the propagation path from the transmitter antenna to the distribution target, the propagation path from the distribution target to the receiving antenna. The functional relationship between parameters and the received power have been discussed [11–13]. The overage power returned from distributed target (e.g., rough surface) that is illustrated by radar is given by:

$$P_r = \iint_A \frac{P_t G^2(\theta, \phi, \theta_0) \sigma^\circ(\theta) \lambda^2}{(4\pi)^3 R^4} dA \tag{1}$$

where θ_0 is the look direction of the bore sight of the Tx/Rx antenna; R is the distance from the antenna to the illustrated area; P_t is the transmitted power; σ° is also called differential radar cross section; G is antenna gain pattern. From Fig. 1, Radar Scattering Plane, then neglecting surface tilt, the differential unit of area on the scattering plane is given by

$$dA = R^2 \frac{\sin\theta}{\cos\theta} d\theta d\phi = R^2 \tan\theta d\theta d\phi \tag{2}$$

Let h be the radar to target distance at normal incidence, then

$$R = \frac{h}{\cos q} \tag{3}$$

Now, (1) becomes

$$P_r = \frac{P_t \lambda^2}{2(4\pi)^3 h^2} \int_0^{2\pi} \int_0^{\frac{\pi}{2}} G^2(\theta, \phi, \theta_0) sin2\theta\sigma_0(\theta) d\theta d\phi \tag{4}$$

A reference measurement may be taken at normal incidence using a spherical conducting as a target. The return power P_{rcal} from the spherical conducting is directed from (1)

$$P_{rcal} = \frac{P_{tcal}\lambda^2}{(4\pi)^3 (R_{cal})^4} G^2(\theta, \phi, \theta_0) \sigma_{cal} \tag{5}$$

$$P_{rcal} = \frac{P_{tcal}\lambda^2 \pi r_{cal}^2}{(4\pi)^3 (R_{cal})^4} G^2(\theta,\phi,\theta_0) \tag{6}$$

r_{cal} is the radius of spherical conducting.

Equation (4) may be normalized by division by (6), yielding the normalized average power

$$P_r = K \int_0^{2\pi} \int_0^{\frac{\pi}{2}} g^2(\theta, \phi, \theta_0) \sin 2\theta \sigma^0(\theta) d\theta d\phi \tag{7}$$

$$g^2(\theta, \phi, \theta_0) = \frac{G^2(\theta, \phi, \theta_0)}{G^2(\theta, \phi, \theta_0)} \tag{8}$$

$$g^2(0, 0, 0) = 1 \tag{9}$$

$$K = \frac{P_{rcal} P_t R_{cal}^4}{2\pi r_{cal}^2 P_{tcal} h^2} \tag{10}$$

P_{tcal} is the transmitted power, R_{cal} is the distance from the antenna to the spherical conducting.

The reference measurement in anechoic chamber is shown in Fig. 2. The coherent radar system is a wideband measurement system can be used to suppress much of the background through range gating of the return signal. This is done by using a reflection signal waveforms, the reflection signal form is shown Fig. 3.

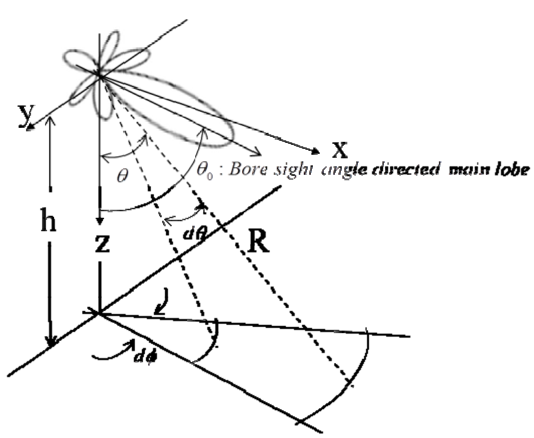

Figure 1: Radar scattering plane.

Figure 2: Reference measurements in anechoic chamber.

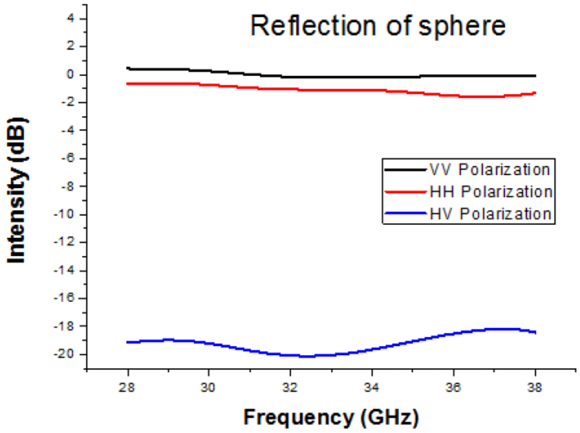

Figure 3: Recorded spectral data.

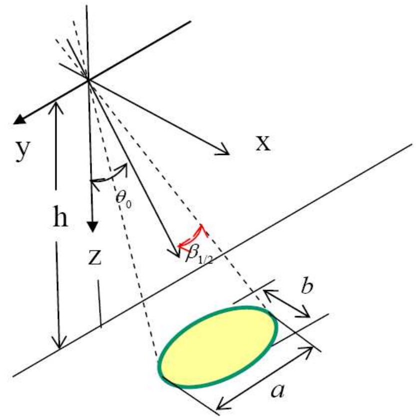

Figure 4: Narrow beam and constant gain pattern (circular beam with beam-width).

The narrow beam and constant gain pattern is shown Fig. 4.

$$a \approx \frac{2R\beta_{1/2}}{\cos\theta_0} = \frac{2\beta_{1/2}h}{\cos^2\theta_0} \tag{11}$$

$$b \approx 2R\beta_{1/2} = \frac{2h\beta_{1/2}}{\cos\theta_0} \tag{12}$$

$$A = \pi\frac{a}{2}\frac{b}{2} = \frac{\pi}{4}ab \approx \frac{\pi\beta_{1/2}^2h^2}{\cos^3\theta_0} \tag{13}$$

$$s^0 = \frac{P_r}{P_{rcal}}\frac{P_{tcal}}{P_t}\frac{h^2r_{cal}^2}{R_{cal}^4b_{1/2}^2\cos q_0} \tag{14}$$

3. MEASUREMENT SETUP

Backscattering measurements of tree canopy have been made with the coherent radar system mounted on the top of a 15 m-height roof. The platforms provide different, but complementary information about backscattering measurements statistics of tree canopy. Because of the relatively small footprint of its antenna narrow beam approximation, the platform-mounted coherent radar system is well suited for making observation of the selected tree targets, and the radar measurements can be arranged with detailed ground truth information about the tree targets.

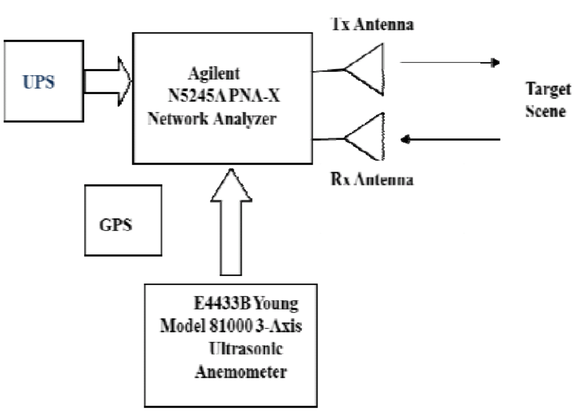

Figure 5: A simplified block diagram of the coherent radar system.

Figure 6: A agilent N5245A PNA-X network analyzer.

Figure 7: Test site as seen from the dish antenna.

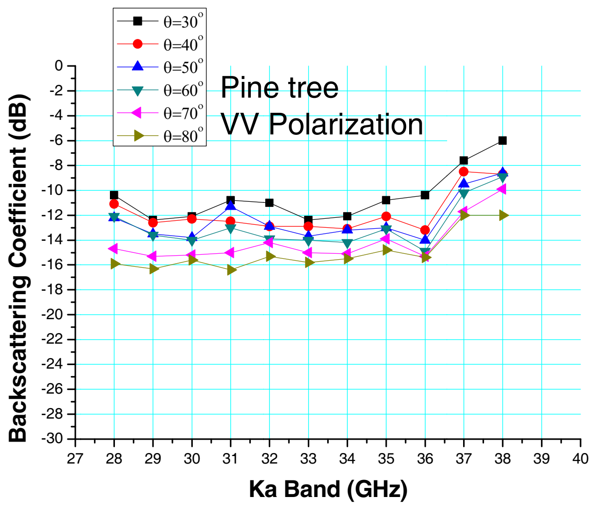

Figure 8: Backscattering coefficient of pine tree from 28 GHz to38 GHz for VV polarization.

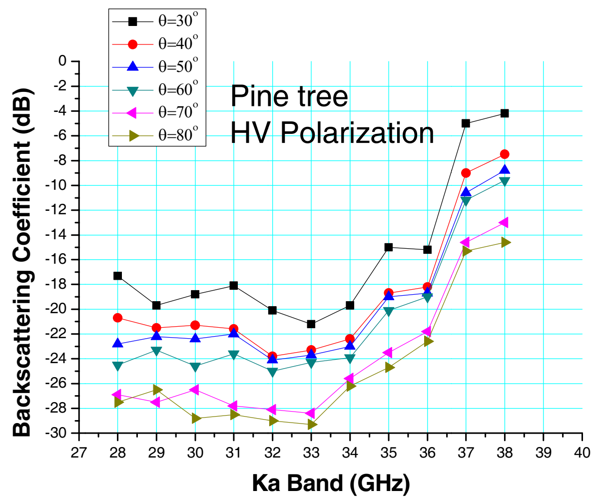

Figure 9: Backscattering coefficient of pine tree from 28 GHz to 38 GHz for HV polarization.

The coherent radar system is not very flexible, but it is discussed in some detail to illustrate calibration techniques also apply to the complex system. Fig. 5 shows a simplified block diagram of the coherent radar system, designed and configured based on a vector network analyzer N5245A PNAX (10 MHz–50 GHz), and the vector network analyzer is shown in Fig. 6.

The current backscattering measurements of tree canopy at Kaband are presented [14, 15]. The measurements show different backscattering behaviors for different tree configurations. The intention of the backscatter experiments is to research the effects of various tree components In Fig. 7 shows the test site as seen from the dish antenna, pine and banyan tree were selected for this study, the Ka band backscattering measurements were conducted on a single banyan tree and other single pine tree on National Central University (NCU) campus.

4. MEASUREMENT AND DISCUSSION

Figures 8–10 plots the backscattering coefficients of pine tree from 28 GHz to38 GHz for VV, HV and HH polarizations, respectively, with angle of incidence from 30 to 80 degrees. The other set of the plots are Figs. 11–13 for banyan tree. At Ka band, wavelength (1.1 cm $\sim$ 0.7 cm) is much smaller than most leaves and branches. For banyan tree, the leaf stems constitute a very small percentage of visible surfaces and may be reasonably ignored. In pine tree, the leaf stems constitute a large percentage of the visible surface, and contributions from multiple scattering reflections are larger than banyan trees. The interested factors that affect the properties of backscattering include frequency, polarization, incident angle, and canopy parameters. In viewing these figures, it can be seen that the cross-polarized returns generally presents higher dynamic range over the frequency and angular behavior.

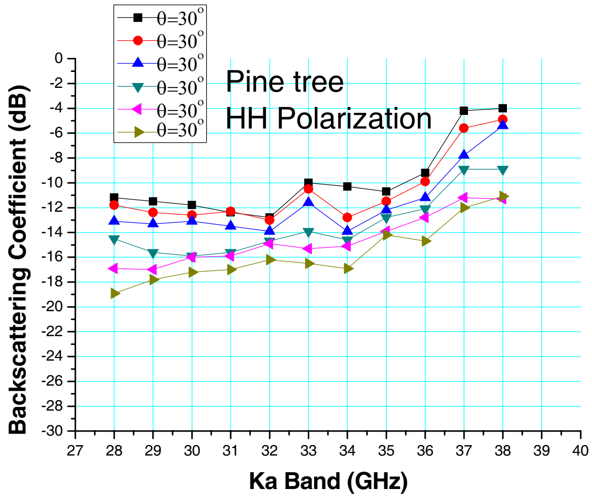

Figure 10: Backscattering coefficient of pine tree from 28 GHz to 38 GHz for HH polarization.

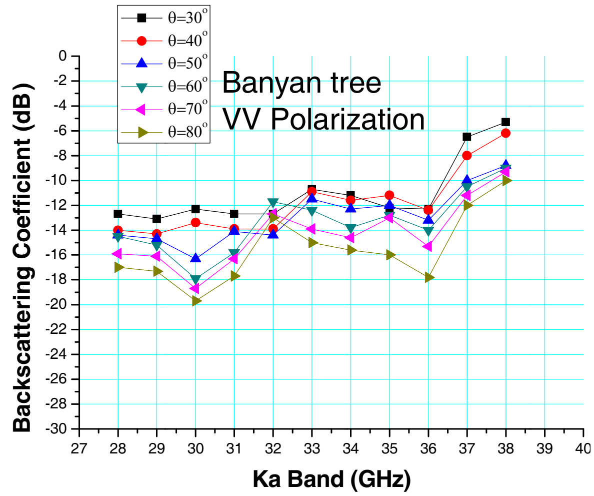

Figure 11: Backscattering coefficient of banyan tree from 28 GHz to 38 GHz for VV polarization.

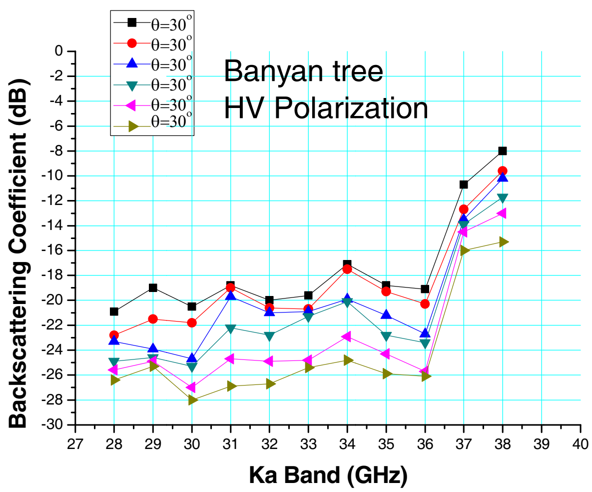

Figure 12: Backscattering coefficient of banyan tree from 28 GHz to 38 GHz for HV polarization.

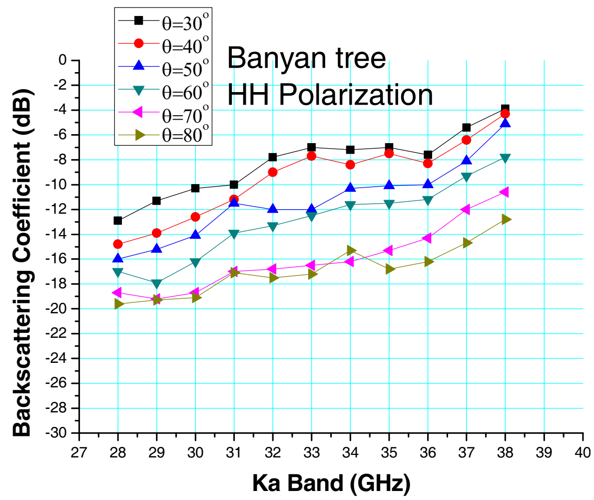

Figure 13: Backscattering coefficient of banyan tree from 28 GHz to 38 GHz for HH polarization.

5. CONCLUSION

We have measured the backscattering coefficient of trees using the coherent radar for VV, HH, HV polarizations at incidence angles between 20 and 80 degrees. The applicability of the technique to measurement of backscattering and extinction in tree canopies, we have modified and established the measured Equation (14) was verified experimentally by conducting two sets of indoor and outdoor measurements on banyan and pine tree. Ground truth measurements were made concurrently with backscatter measurements to establish a physical relationship between tree canopy parameters and the backscattering measured.

REFERENCES

1. Ulaby, F. T., R. K. Moore, and A. K. Fung, *Microwave Remote Sensing: Radar Remote Sensing*, Vol. 2, Artech House, Deham, MA, 1982.
2. Fung, A. K. and K. S. Chen, *Microwave Scattering and Emission Models for Users*, Artech House, Norwood, MA, 2010.
3. Ulaby, F. T. and M. C. Dobson, *Handbook of Radar Scattering Statistics for Terrain*, Artech House, MA, 1989.
4. Ruck, G. T., D. E. Barrick, W. D. Stuart, and C. K. Krichbaum, *Radar Cross Section Handbook*, Plenum Press, New York, 1970.

5. Ishimaru, A., *Wave Propagation and Scattering in Random Media*, Academic Press, San Francisco, CA, 1978.
6. Tsang, L., J. A. Kong, and R. T. Shin, *Theory of Microwave Remote Sensing*, John Wiley, New York, 1985.
7. Ulaby, F. T., R. K. Moore, and A. K. Fung, *Microwave Remote Sensing: Fundamentals and Radiometry*, Vol. 1, Artech House, Deham, MA, 1981.
8. Ulaby, F. T., R. K. Moore, and A. K. Fung, *Microwave Remote Sensing: From Theory to Applications*, Vol. 3, Artech House, Deham MA, 1986.
9. Ulaby, F. T., R. K. Moore, and A. K. Fung, *Microwave Remote Sensing: Radar Remote Sensing*, Vol. 2, Artech House, Deham, MA, 1982.
10. Fung, A. K. and K. S. Chen, *Microwave Scattering and Emission Models for Users*, Artech House, Norwood, MA, 2010.
11. Ulaby, F.T., and Dobson, M. Craig, *Handbook of Radar Scattering Statistics for Terrain*, Artech House, MA, 1989.
12. Ruck, G. T., D. E. Barrick, W. D. Stuart, and C. K. Krichbaum, *Radar Cross Section Handbook*, Plenum Press, New York, 1970.
13. Knott, E. F., J. F. Shaeffer, and M. T. Tuley, *Radar Cross Section*, Artech House, MA, 1993.
14. Kim, H., J. T. Johnson, and B. A. Baertlein, "Ka band backscatter measurements and modeling of tree foliage," *1998 IEEE International Geoscience and Remote Sensing Symposium Proceedings, 1998. IGARSS '98*, Vol. 4, 2086-2088, 1998.
15. Kim, H., J. T. Johnson, and B. A. Baertlein, "High resolution Ka-band images of a small tree: Measurements and models," *IEEE Transactions on Geoscience and Remote Sensing*, Vol. 38, 899–910, 2000.